JOURNAL OF MATERIALS SCIENCE **34** (1999) 3307–3314

Kinetic studies on hot-stretching of polyacrylonitrile-based carbon fibres by using internal resistance heating

Part II *Changes in structure and mechanical properties*

HONG SU KIM, M. SHIOYA*
Department of Organic and Polymeric Materials, Tokyo Institute of Technology, 2-12-1 O-okayama, Meguro-ku, Tokyo 152, Japan
E-mail: mshioya@o.cc.titech.ac.jp

A. TAKAKU
Department of Life Culture, Seitoku University, 531 Sagamidai, Matsudo-shi, Chiba 271, Japan

The effects of the stretching stress applied during high-temperature heat treatment of polyacrylonitrile-based carbon fibres on the development of the structure and the mechanical properties of the resulting carbon fibres, were investigated kinetically by using internal resistance heating. The tensile modulus of the carbon fibres increased with a faster rate under a larger stretching stress. The tensile strength decreased initially as the carbonization progressed, but increased appreciably under a larger stretching stress, a trend which was not observed under a smaller stretching stress. The temperature–time superposition was applicable with respect to the development of the crystallite and the microvoid structures and the changes in the resistivity, density and apparently the tensile strength, by using a common shift factor. The changes in the longitudinal strain, however, showed a different temperature dependence from that of the structural development.
© *1999 Kluwer Academic Publishers*

1. Introduction

In the conventional process to produce polyacrylonitrile(PAN)-based carbon fibres, PAN is converted to carbon by a low-temperature heat treatment to stabilize thermally the starting fibres and a high-temperature heat treatment to carbonize the stabilized fibres. The resulting carbon fibres consist of crystallites having highly anisotropic elastic properties. Thus, the degree of preferential orientation of the crystallites is a dominant factor determining the tensile modulus of the carbon fibres [1]. The tensile modulus of the PAN-based carbon fibres tends to increase with increasing carbonization temperature owing to the development of oriented carbon structure. On the other hand, the tensile strength tends to decline when heat treatment at a higher temperature is applied [2, 3]. In order to obtain higher tensile modulus without loss in tensile strength, it is effective to apply stretching stress during the higher temperature heat treatment [4]. The effects of the hot-stretching on the development of the structure and the mechanical properties of the resulting carbon fibres have been investigated on pitch-based [5, 6] and PAN-based [7, 8] carbon fibres.

The present study kinetically investigated the effects of stretching stress applied during high-temperature heat treatment of PAN-based carbon fibres. The heat treatments were carried out using an internal resistance heating [9–14] by taking account of the advantages for this study; that is, the ability to extend the heat-treatment time to the shorter region and the ability to obtain accurate values of the strain induced by the stretching stress. In Part I of this study [15], the effects of the stretching stress on the carbonization behaviour have been analysed from the resistivity changes taking place during the heat treatment. The temperature–time superposition has been applied to the resistivity changes under stretching stress. The carbonization behaviour has been treated as a superposition of the first-order rate processes with distributed rate constants having a single value of the activation energy. It has been shown that the application of the stretching stress effectively reduces the activation energy in the temperature region below 1800 °C, and diminishes the fractions of the slower rate processes.

This paper reports the effects of the stretching stress on the development of the structure and the

* Author to whom all correspondence should be addressed.

mechanical properties of the resulting PAN-based carbon fibres. The microvoid structure in the carbon fibres will be analysed with the small-angle X-ray scattering (SAXS) using a method proposed by the present authors [16–18], which takes account of the anisotropy of the microvoid structure.

2. Experimental procedure

2.1. Fibres

The PAN-based carbon fibres processed at about 1250 °C at maximum, were used for the starting fibres of the internal resistance heating. These fibres were in the form of a tow comprising 3000 continuous filaments. The tensile modulus and the strength of the fibres are 255 and 3.92 GPa, respectively.

2.2. Internal resistance heating

A carbon fibre tow was extended in a Pyrex glass tube in contact with four graphite pulleys, and the tow was resistance heated by using a pair of inner pulleys, 10 cm apart, as electrodes. A constant tension was applied to the tow by suspending a dead weight on one end of the tow. The extension of the tow was detected by using a pulley and angular detector. The quoted value of the heat-treatment temperature is the surface temperature of the tow which was measured by using an infrared radiation thermometer (Minolta IR-630) from outside of the glass tube. Nitrogen gas was flowed in the glass tube at a rate of 51 min^{-1}. In order to bind closely the filaments in the tow, a twist of one turn per 5 cm was given to the tow.

The heat treatments were carried out according to the following procedure. First, a tow was heat treated at 600 °C for 30 min for conditioning. After the tow was cooled down to a room temperature, a dead weight of desired mass was suspended on the tow. Then, the tow was has heat treated in two different ways. For the isothermal heat treatment, the tow was heated up to a desired temperature instantaneously, and was kept at this temperature for a desired duration. For the heat treatment with increasing temperature conditions, the tow was heated at a rate of 100 °C min^{-1} up to the desired temperature and was kept at this maximum temperature for 1 min. For both heat treatments, the electric power was turned off immediately after the heat treatment was finished, and the tow was left to cool in the heating apparatus down to room temperature within a few seconds.

2.3. Measurements

2.3.1. Wide-angle X-ray diffraction

The wide-angle X-ray diffraction (WAXD) from the crystallites in the heat-treated carbon fibres was measured at room temperature by using a diffractometer (Rigaku denki) and nickel-filtered CuK_α radiation. The X-ray specimens were prepared by aligning the carbon fibres parallel to each other to form a rectangular cross-section.

The equatorial 0 0 2 and the meridional 1 0 diffraction intensity distributions were measured as a function of the diffraction angle by using a position-sensitive proportional counter (PSPC). The interlayer spacing, d_{002}, was calculated from the peak diffraction angle of the 0 0 2 diffraction by using the Bragg equation. The layer stacking height, L_c, and layer extent in the fibre axis direction, L_a, were calculated from the width of the 0 0 2 and the 10 diffractions by using the Scherrer equation and an equation proposed by the present authors [18], respectively.

The 0 0 2 diffraction intensity distribution was measured as a function of the azimuthal angle by using a Geiger counter and a goniometer with a symmetrical transmission geometry. From the full-width at half-maximum intensity of the peak, $\Delta\phi$, the orientation parameter, f, was calculated as follows

$$f = 1 - \frac{\Delta\phi}{\pi} \tag{1}$$

2.3.2. Small-angle X-ray scattering

The small-angle X-ray scattering from the microvoids in the heat-treated carbon fibres was measured at room temperature on the same specimens used for the WAXD measurements. The incident CuK_α X-ray beam was collimated with two pin-holes of 0.3 and 0.5 mm diameter. The sample-to-detector distance was 360 mm. The scattering intensity was measured by using the PSPC with a pulse-height discriminator. No height-limiting slit was attached to the entrance window of the PSPC.

By analysing the equatorial intensity distributions, the average area of the microvoid cross-sections in a plane perpendicular to the fibre axis, S_3, and the microvoid volume fraction, v_p, were calculated according to a method proposed by the present authors [16–18].

2.3.3. Density

The density of the heat-treated carbon fibres was measured at 30 °C with a sink–float method using mixtures of carbon tetrachloride and ethylene dibromide.

2.3.4. Longitudinal strain

The longitudinal strain of the carbon fibres, ε, on the basis of the initial fibre length, which was induced during heat treatment, was calculated by using the equation [15]

$$\varepsilon = \exp\left(\frac{\Delta L}{L}\right) - 1 \tag{2}$$

where L is the distance between the electrodes and ΔL the increase in the length of the fibres in the hot zone.

2.3.5. Mechanical properties

The sonic propagation velocity in the heat-treated carbon fibre tows was measured in free state at room temperature by using a transmitter and a receiver made of piezotransducers and 1 MHz ultrasonic waves. The sonic modulus of the fibres in the fibre axis direction,

E_s, was calculated from the sonic propagation velocity, C, and the fibre density, ρ, as follows

$$E_s = \rho C^2 \tag{3}$$

The tensile strength of the heat-treated carbon fibres was measured at room temperature by using single-fibre tensile tests with a tensile tester. The gauge length was 10 mm and the crosshead speed was 0.4 mm min^{-1}. Quoted values of the tensile strength are the averages of at least 17 determinations on individual fibres.

The fibre diameter required for calculating tensile strength was determined from the diffraction of the He–Ne laser beam by individual fibres. The fibre diameter, D, was calculated by using the equation

$$D = \frac{\lambda}{2 \sin \theta} \tag{4}$$

where λ is the wavelength of the laser beam, and 2θ is the scattering angle of the intensity minimum of the first order.

3. Results and discussion

3.1. Structural development

According to the temperature–time superposition adopted in the phenomenological treatment of the carbonization behaviour [19], the heat-treatment time, t, at an arbitrary temperature, T, is equivalent to the heat-treatment time, t_0, at a reference temperature, T_0, where t_0 is related to t by the equation

$$t_0 = \kappa(T)t \tag{5}$$

The coefficient $\kappa(T)$ depends only on the heat-treatment temperature. In Part I of this study [15], it has been shown that the temperature–time superposition can be applied to the resistivity changes taking place during heat treatment of PAN-based carbon fibres under a constant stretching stress. Smooth composite curves at a reference temperature over a wide range of heat-treatment times have been constructed by shifting the isothermal resistivity versus $\log_{10}t$ diagrams at various temperatures along the $\log_{10}t$ axis by the amount $\log_{10}\kappa(T)$. The shift factors, $\log_{10}\kappa(T)$, used to superimpose resistivity changes referring to a temperature of 1200 °C are plotted against the heat-treatment temperature in Fig. 1.

For the high-temperature heat treatment of PAN- and pitch-based carbon fibres, the temperature–time superposition can be applied with respect to the development of the crystallite and microvoid structures and changes in the density by using the shift factor which was determined from the resistivity changes [13]. Thus, if the shift factor for the resistivity changes is known, the changes in structural parameters over decades of time scale at a reference temperature can be obtained from the limited number of the measurements of the structural parameters.

In the present study, the interlayer spacing, d_{002}, the layer stacking height, L_c, the layer extent in the fibre

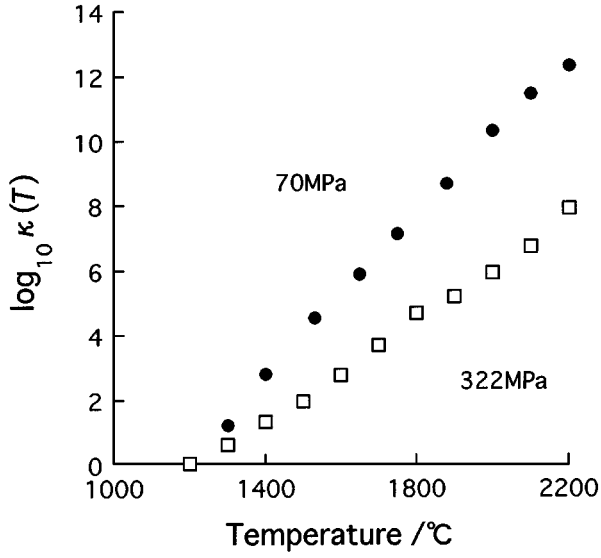

Figure 1 Shift factor, $\log_{10}\kappa(T)$, used to superimpose resistivity changes referring to temperature of 1200 °C versus heat-treatment temperature, T. Stretching stresses are shown in the figure.

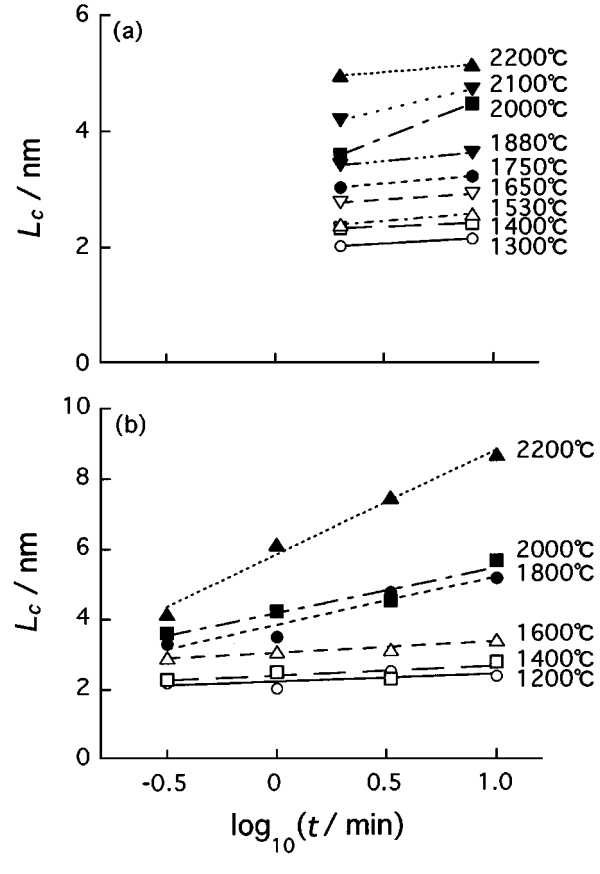

Figure 2 Layer stacking height, L_c, of crystallites in isothermally heat-treated carbon fibres versus heat-treatment time, t. Stretching stresses are (a) 70 and (b) 322 MPa and heat-treatment temperatures are shown in the figure.

axis direction, L_a, and the orientation parameter, f, were measured for the crystallites in the PAN-based carbon fibres isothermally heat treated at various temperatures under stretching stresses of 70 and 322 MPa. The changes in the layer stacking height, for example, are shown in Fig. 2. The values of the heat-treatment time, t, were converted to the reduced time, $\kappa(T)t$, by

using the values of $\kappa(T)$ shown in Fig. 1. Thus the obtained composite curves of these structural parameters referred to a temperature of 1200 °C are shown in Figs 3–5. Because smooth composite curves are obtained, it is known that the structure of the carbon fibres evolves following the same thermally activated kinetic process that induces resistivity changes. It is seen that the crystallite sizes and the orientation develop with much faster rates under a larger stretching stress.

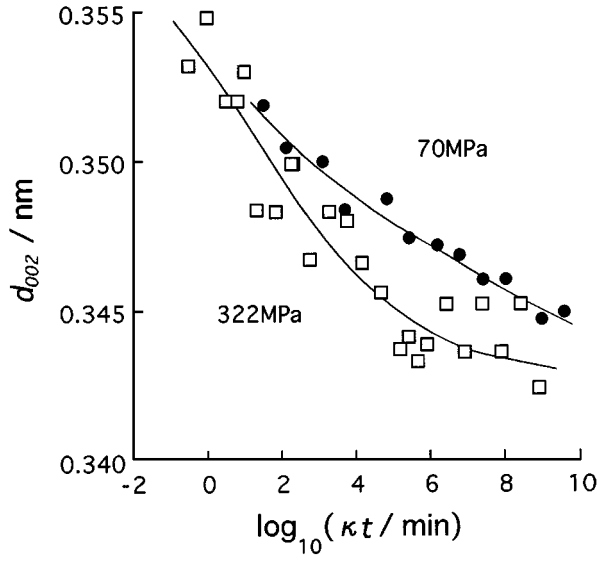

Figure 3 Composite curves of interlayer spacing, d_{002}, of crystallites in carbon fibres isothermally heat treated at 1200 °C versus reduced time, $\kappa(T)t$. Stretching stresses are shown in the figure.

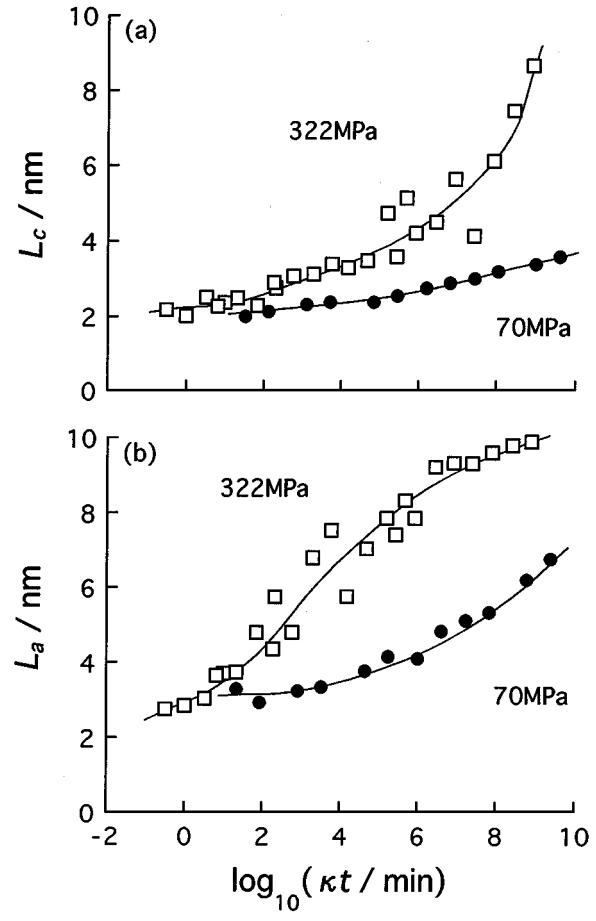

Figure 4 Composite curves of (a) layer stacking height, L_c, and (b) layer extend in the fibre axis direction, L_a, of crystallites in carbon fibres isothermally heat treated at 1200 °C versus reduced time, $\kappa(T)t$. Stretching stresses are shown in the figure.

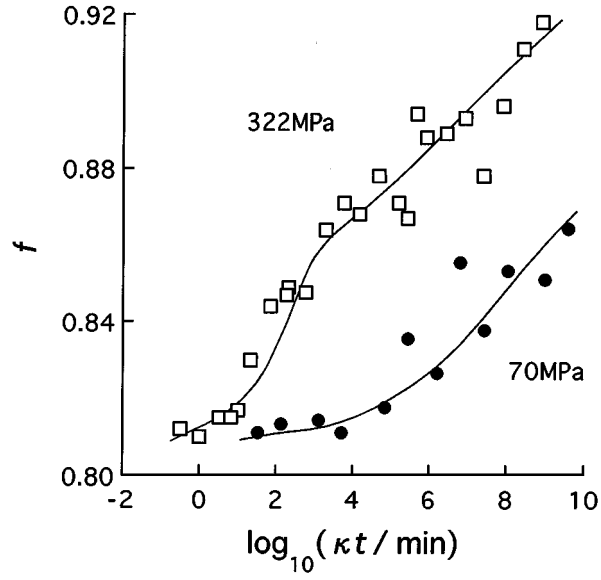

Figure 5 Composite curves of orientation parameter, f, of crystallites in carbon fibres isothermally heat treated at 1200 °C versus reduced time, $\kappa(T)t$. Stretching stresses are shown in the figure.

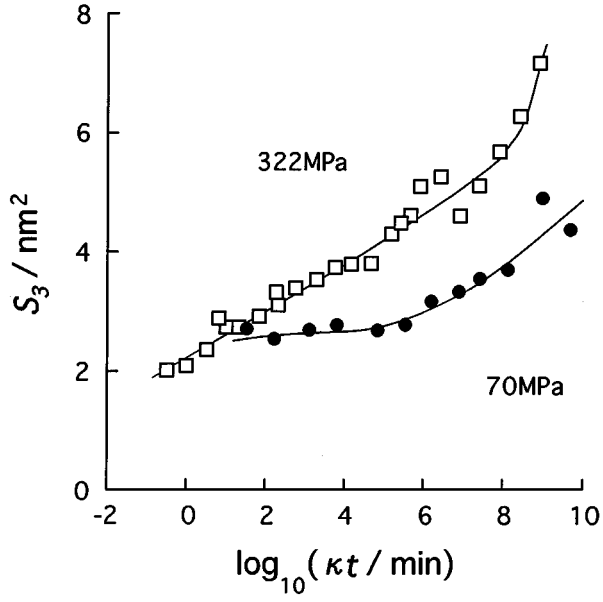

Figure 6 Composite curves of the average area of microvoid cross-sections in a plane perpendicular to the fibre axis for carbon fibres isothermally heat-treated at 1200 °C versus reduced time, $\kappa(T)t$. Stretching stresses are shown in the figure.

The composite curves of the average microvoid cross-sectional area, S_3, referred to a temperature of 1200 °C, are shown in Fig. 6. The microvoid cross-section grows larger with increasing reduced time and under a larger stretching stress.

If the temperature–time superposition using the same shift factor can be applied to different structural parameters, plots of one structural parameter versus another will yield a single curve representing a relation between these two parameters from which the precise temperature–time conditions are eliminated. The microvoid cross-sectional area is plotted against the layer

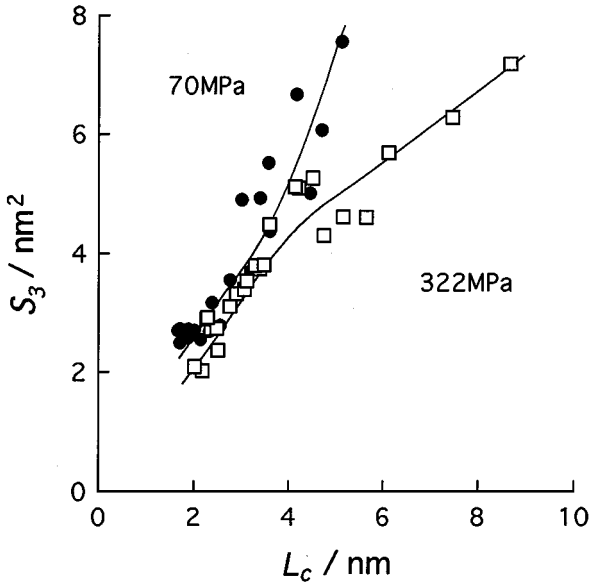

Figure 7 Average area of microvoid cross-sections in a plane perpendicular to fibre axis, S_3, in carbon fibres isothermally heat treated with various temperature–time conditions versus layer stacking height, L_c, of crystallites. Stretching stresses are shown in the figure.

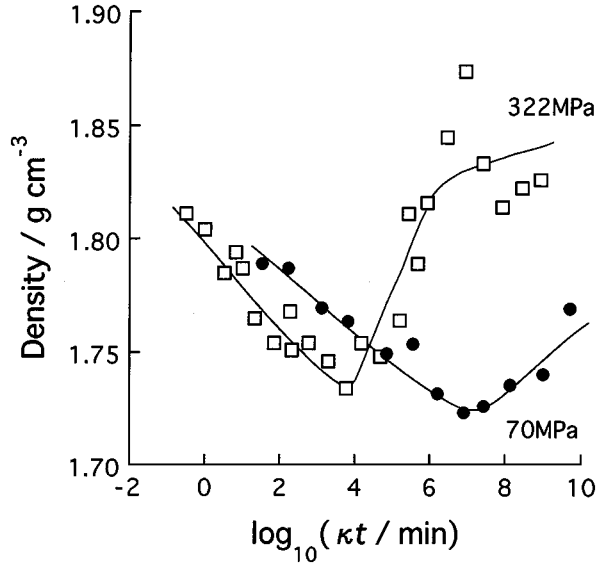

Figure 9 Composite curves of the density of carbon fibres isothermally heat treated at 1200 °C versus reduced time, $\kappa(T)t$. Stretching stresses are shown in the figure.

stacking height in Fig. 7. The microvoid cross-section tends to increase as the layer stacking height increases. No significant difference attributed to the stretching stress is found up to the layer stacking height of 4 nm. In the region where the layer stacking height grows larger than 4 nm, however, the effect of the stretching stress is clearly discerned. At an equivalent layer stacking height, the microvoid cross-section becomes appreciably smaller when a larger stretching stress is applied.

The composite curves of the microvoid volume fraction, v_p, referred to a temperature of 1200 °C, are shown in Fig. 8. For both stretching stresses of 70 and 322 MPa, the microvoid volume fraction initially increases with increasing reduced time. When the reduced time passes 10^4 min, the effect of the stretching stress becomes noticeable. The microvoid volume fraction continues to increase under the stretching stress of 70 MPa, while it begins to decrease under the stretching stress of 322 MPa.

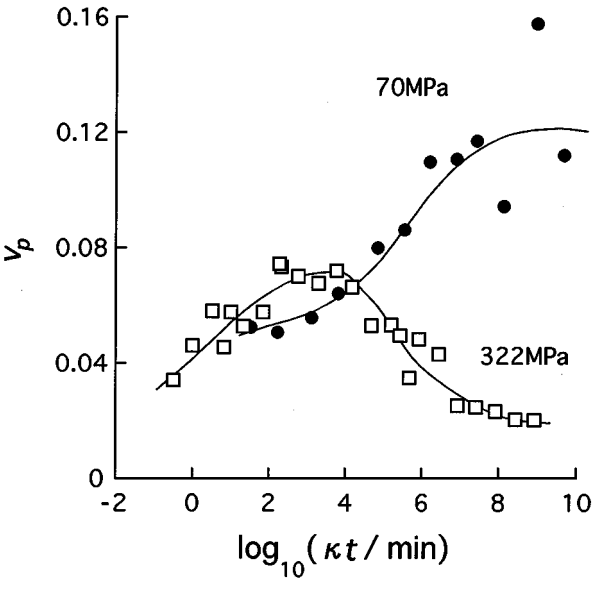

Figure 8 Composite curves of microvoid volume fraction, v_p, in carbon fibres isothermally heat treated at 1200 °C versus reduced time, $\kappa(T)t$. Stretching stresses are shown in the figure.

The composite curves of the fibre density referred to a temperature of 1200 °C are shown in Fig. 9. The fibre density initially decreases with increasing reduced time, and after reaching a minimum, it begins to increase. The reduced time at which the fibre density reaches a minimum is decreased by applying a larger stretching stress. By comparing Figs 8 and 9, the increase in the fibre density in the reduced time region longer than 10^4 min, found for the stretching stress of 322 MPa, can be related to the decrease in the microvoid volume fraction in this reduced time region. It was found that, when the density was corrected for the microvoid volume fraction, that is, the density was divided by $1 - v_p$, the minima in the density changes disappeared for both stretching stresses, and the increase in the density due to the densification of the materials was revealed.

3.2. Changes in mechanical properties

The sonic modulus of the carbon fibres heat treated with increasing temperature conditions is plotted against the maximum heat treatment temperatures in Fig. 10. It has been shown that the sonic modulus of the carbon fibres determined with the method used in this study coincides with the modulus determined from the tensile tests [20]. For both stretching stresses of 70 and 322 MPa, the fibre modulus increases with increasing heat-treatment temperature. A marked increase in the fibre modulus is obtained at temperatures above 1800 °C under the stretching stress of 322 MPa.

The tensile strength of the carbon fibres heat treated with increasing temperature conditions is plotted against the maximum heat-treatment temperatures in

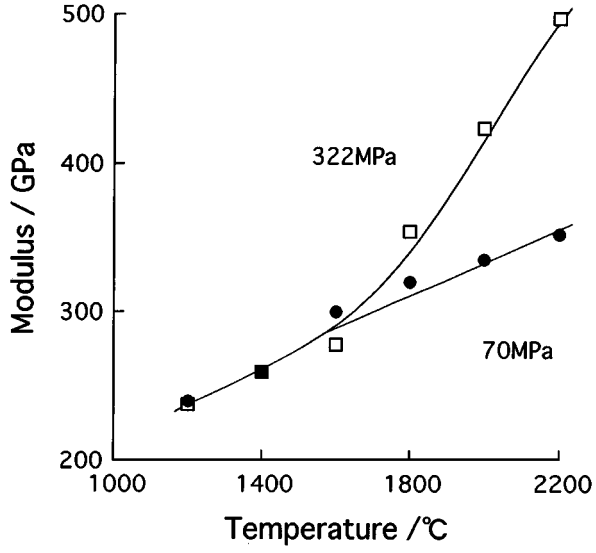

Figure 10 Sonic modulus of carbon fibres heat treated with increasing temperature conditions versus maximum heat-treatment temperature. Stretching stresses are shown in the figure.

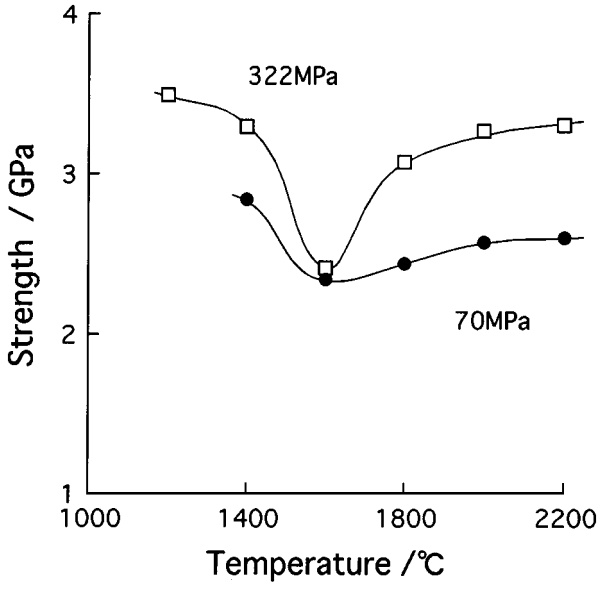

Figure 11 Tensile strength of carbon fibres heat treated with increasing temperature conditions versus maximum heat-treatment temperature. Stretching stresses are shown in the figure.

Fig. 11. At temperatures below 1600 °C, the tensile strength decreases with increasing heat-treatment temperature for both stretching stresses of 70 and 322 MPa. For the stretching stress of 70 MPa, the tensile strength does not change significantly at higher temperatures. For the stretching stress of 322 MPa, however, the tensile strength increases markedly at temperatures above 1800 °C.

The tensile strength of the carbon fibres isothermally heat treated at various temperatures under a stretching stress of 322 MPa is plotted against the heat-treatment time in Fig. 12. In this heat-treatment time region, the tensile strength decreases with increasing heat-treatment time at temperatures below 1600 °C, while it increases above this temperature. This trend is in the same direction as the isochronal changes in the tensile strength with increasing heat-treatment temperature. That is, if the values of the tensile strength shown in Fig. 12 are followed in the order of increasing heat-treatment temperatures at an equivalent heat-treatment time, it is observed that the tensile strength decreases below 1600 °C and then increases above this temperature. This suggests that the temperature–time superposition can be applied with respect to the changes in the tensile strength. By using the shift factors determined from the resistivity changes, the composite curves of the tensile strength referred to a temperature of 1200 °C, were obtained as shown in Fig. 13. It is known that the tensile strength decreases with increasing reduced time up to 10^4 min for both stretching stresses of 70 and 322 MPa. Beyond this reduced time region, the tensile strength increases under the stretching stress of 322 MPa, and the tensile strength of the original carbon fibres is retained. Such a large increase in the tensile strength is not obtained under the stretching stress of 70 MPa.

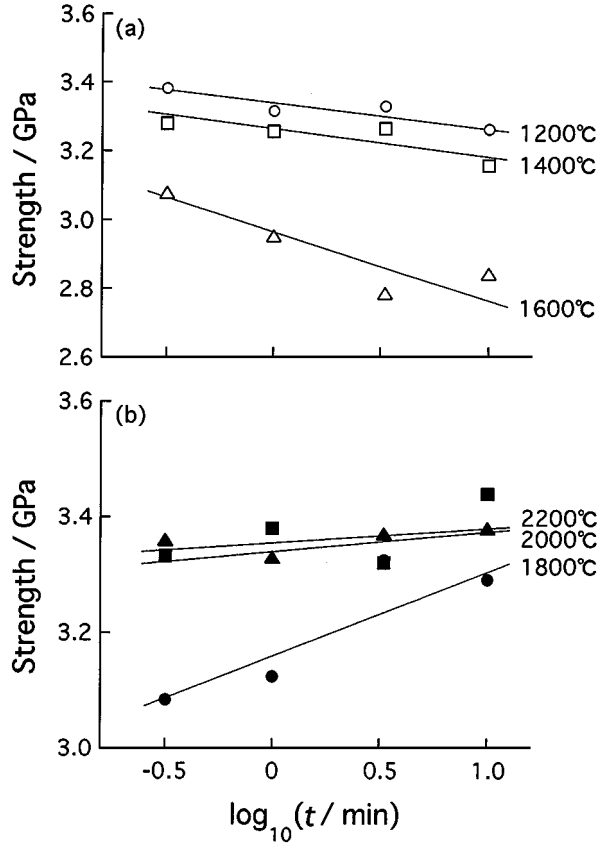

Figure 12 Tensile strength of carbon fibres isothermally heat treated at temperatures (a) below and (b) above 1800 °C versus heat-treatment time, t. The stretching stress is 322 MPa and heat-treatment temperatures are shown in the figure.

3.3. Relation between structure, resistivity, mechanical properties and longitudinal strain

As shown in a previous paper [13], a unique correlation, independent of the kind of starting carbon fibres, exists between the resistivity and the layer extent, L_a. Thus, the temperature–time superposition could be applied with respect to the changes in the structural parameters

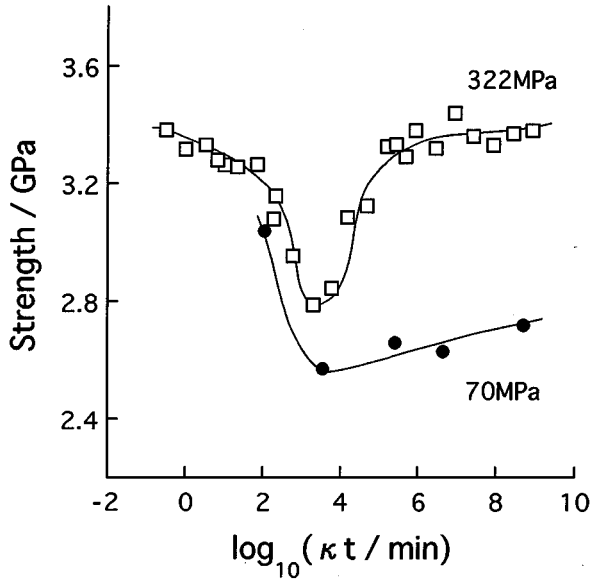

Figure 13 Composite curves of the tensile strength of carbon fibres isothermally heat treated at 1200 °C versus reduced time, $\kappa(T)t$. Stretching stresses are shown in the figure.

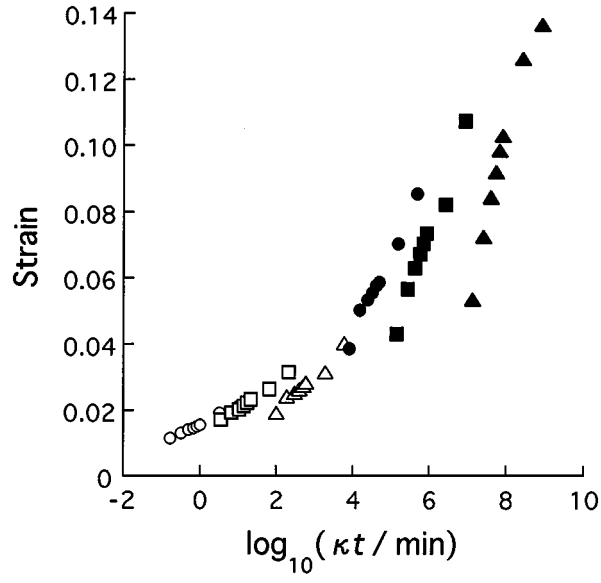

Figure 14 Longitudinal strain of carbon fibres induced during isothermal heat treatments versus reduced time, $\kappa(T)t$, referred to temperature of 1200 °C. Reduced time was calculated using shift factors determined from resistivity changes. The stretching stress is 322 MPa and heat-treatment temperatures are (○) 1200, (□) 1400, (△) 1600, (●) 1800, (■) 2000 and (▲) 2200 °C.

by using the shift factor determined from the resistivity changes.

Because of the anisotropy in the elastic properties of the crystallites in carbon fibres, the crystallite orientation is a crucial factor determining the tensile modulus of the carbon fibres [1]. By comparing Figs 7–9 with 13, the increase in the tensile strength brought about by the stretching stress can be attributed to the smaller microvoid fraction and the smaller sizes of the microvoids as compared with the crystallite sizes. With respect to the crystallite orientation and the microvoid structure, the temperature–time superposition could be applied. Thus, it is considered that the temperature–time superposition could be applied apparently also with respect to the mechanical properties.

In order to compare the longitudinal strain induced during heat-treatment with the structural parameters shown so far in the form of the composite curves, the longitudinal strains shwon in the previous paper [15] are replotted in Fig. 14 on the same time scale as the evolution of the structural parameters. That is, the heat-treatment times at which longitudinal strains were measured were converted to the reduced time by using the shift factors determined from the resistivity changes. It is seen that the relation between the longitudinal strain and the reduced time is temperature dependent and a single relationship is not obtained, which is in contrast with the composite curves of the structural parameters. This suggests that the longitudinal strain involves two components; one being associated with the structural development and the other being independent of the structural development. The temperature dependence of the structure-independent component is different from that of the structural development. Presumably, slip between some structural units such as microfibrils comprising stacks of carbon-layer ribbons, which takes place without causing changes in their structure, may contribute to the structure-independent component of the longitudinal strain.

It has been discussed [19] that the deformation of graphitizing carbons and graphite is a thermally activated kinetic process with the same activation energy as graphitization. For example, an activation energy of 1159 kJ mol^{-1} [21] was obtained from the creep tests on graphite, which is close to the activation energy determined from the structural changes [19]. For these creep tests, a graphite with fine grain size and high density was used, and its structure may be quite different from that of the carbon fibres used in this study. Thus, the difference in the microtexture of carbons significantly influences creep behaviour and the activation energy of the creep deformation.

4. Conclusion

The PAN-based carbon fibres were heat treated with the internal resistance heating by applying stretching stress. The temperature–time superposition using a common shift factor could be applied with respect to the development of the crystallite and the microvoid structures and the changes in the resistivity and the density. Thus, it was known that the structural development and the resistivity changes take place following the same thermally activated kinetic process. The tensile modulus of the carbon fibres increased at a faster rate under a larger stretching stress. For the isothermal heat treatments, the tensile strength decreased initally with increasing heat-treatment time, irrespective of the stretching stresses. Then, the tensile strength began to increase appreciably under a larger stretching stress, a trend which was not observed under a smaller stretching stress. The tensile strength of the carbon fibres was closely related to the microvoid structure. Thus, the temperature–time superposition could be applied apparently to the changes in the tensile strength. The effects of the stretching stress on the tensile strength

were also found for the heat treatment with increasing temperature rate of 100 °C min^{-1}. The tensile strength decreased on heat treatment below 1600 °C, while it increased markedly on heat treatment above 1800 °C under a stretching stress of 322 MPa. The changes in the longitudinal strain showed a different temperature dependence from that of the structural development.

References

1. W. RULAND, *Appl. Polym. Symp*. **9** (1969) 293.
2. R. MORETON, W. WATT and W. JOHNSON, *Nature* **213** (1967) 690.
3. J. W. JOHNSON, *Appl. Polym. Symp*. **9** (1969) 229.
4. J. W. JOHNSON, J. R. MARJORAM and P. G. ROSE, *Nature* **221** (1969) 357.
5. H. M. HAWTHORNE, *J. Mater. Sci*. **11** (1976) 97.
6. H. M. HAWTHORNE, in "Proceedings of the International Conference on Carbon Fibers and their Composites" (Plastics Institute, London, 1971), p. 81.
7. D. H. ISAAC, S. OZBEK and J. G. FRANCIS, *Mater. Manuf. Process*. **9** (1994) 179.
8. S. OZBEK and D. H. ISAAC, *ibid*. **9** (1994) 199.
9. D. J. PINCHIN and R. T. WOODHAMS, *J. Mater. Sci*. **9** (1974) 300.
10. K. YAMAMOTO, T. KIKUTANI and A. TAKAKU, *Tanso* (*Jpn*) **146** (1991) 8.
11. T. KIKUTANI, K. YAMAMOTO and A. TAKAKU, *ibid*. **148** (1991) 142.
12. A. TAKAKU, T. MANGANZI and M. SHIOYA, *ibid*. **163** (1994) 119.
13. A. TAKAKU, M. SHIOYA and T. MANGANZI, *Carbon* **34** (1996) 1449.
14. H. S. KIM, M. SHIOYA and A. TAKAKU, *J. Mater. Sci*. **34** (1999) 3299.
15. *Idem., ibid*. **34** (1999) 3299.
16. M. SHIOYA and A. TAKAKU, *J. Appl. Phys*. **58** (1985) 4074.
17. A. TAKAKU and M. SHIOYA, *J. Mater. Sci*. **21** (1986) 4443.
18. *Idem., ibid*. **25** (1990) 4873.
19. D. B. FISCHBACH, in "Chemistry and Physics of Carbon," edited by P. L. Walker Jr (Dekker, New York, 1968) Vol. 7, pp. 1–105.
20. E. HAYAKAWA, M. SHIOYA and A. TAKAKU, *Adv. Compos. Mater*. **4** (1994) 33.
21. G. M. JENKINS, *Philos. Mag*. **8** (1963) 903.

Received 30 June 1997
and accepted 13 February 1998